Journal of Physiology (1992), **450**, *pp.* 593–611
With 12 figures
Printed in Great Britain

THE MINIMAL INHIBITORY SYNAPTIC CURRENTS EVOKED IN NEONATAL RAT MOTONEURONES

BY TOMOYUKI TAKAHASHI

From the Department of Physiology, Kyoto University Faculty of Medicine, Kyoto 606, Japan

(*Received 6 March 1991*)

SUMMARY

1. Tight-seal whole-cell recordings were made from lumbar motoneurones visually identified in thin slices of neonatal rat spinal cord. The inhibitory postsynaptic currents (IPSCs) were evoked by extracellular stimulation of a neighbouring internuncial neurone in the presence of glutamate receptor antagonists.

2. Glycinergic IPSCs were recorded in the presence of bicuculline. The IPSCs appeared in an all-or-none manner as the graded stimulus intensity exceeded a certain threshold. Their latencies showed a unimodal distribution with a mean of 0·81 ms at 37 °C. Thus, the observed IPSCs are suggested to be monosynaptically evoked unitary IPSCs. The mean conductance of unitary IPSCs was $2·9 \pm 1·2$ nS ($\pm$S.D.).

3. When the external Ca^{2+} concentration ($[Ca^{2+}]_o$) was reduced, the number of failures in response to stimulation increased, thereby reducing the mean amplitude of IPSCs. The mean amplitude of IPSCs was linearly related to the $[Ca^{2+}]_o$ (0·35–1·4 mM) with a mean slope of $3·1 \pm 0·67$ on double logarithmic co-ordinates.

4. The amplitude of individual IPSCs decreased with decrease in $[Ca^{2+}]_o$. However, below 0·7 mM $[Ca^{2+}]_o$, the mean amplitude of IPSCs (excluding failures) reached a steady minimum level. The mean conductance of these IPSCs measured in 0·5 mM $[Ca^{2+}]_o$ was 657 ± 281 pS.

5. The minimal IPSCs had a coefficient of variation of $0·50 \pm 0·13$. No clear correlation was observed between the rise time and the amplitude of minimal IPSCs evoked in individual motoneurones, indicating that the amplitude variability is not due to the different synaptic locations.

6. Spontaneous miniature IPSCs were recorded from motoneurones in the presence of tetrodotoxin. The miniature IPSCs had a mean conductance of 739 ± 278 pS, being comparable to the minimal evoked IPSCs.

7. Under various internal and external Cl^- concentration, the reversal potential of the IPSCs (E_{IPSC}) approximately coincided with the Cl^- equilibrium potential. A 730-fold change in the potassium concentration gradient across the membrane did not affect the E_{IPSC}. The permeability ratio of K^+ to Cl^- (P_K/P_{Cl}) was less than 0·05.

8. It is concluded that the IPSCs are carried almost exclusively by Cl^- and that the minimal evoked IPSCs represent the quantal response of the transmitter.

MS 9209

INTRODUCTION

The quantal hypothesis of transmitter release was proposed by del Castillo & Katz (1954) in the amphibian neuromuscular junction. Kuno and his colleagues extended this hypothesis to central synapses by showing that the amplitude fluctuations of synaptic potentials in spinal motoneurones can be described by Poisson or binomial statistics (Kuno, 1964, 1971; Kuno & Weakly, 1972). Using the deconvolution method, Redman and his colleagues reported that the amplitude fluctuations of excitatory postsynaptic potentials (EPSPs) recorded from cat central neurones cannot be described by a single Poisson or binomial model because of the non-uniform release probability at individual release sites (Edwards, Redman & Walmsley, 1976; Jack, Redman & Wong, 1981; Walmsley, Edwards & Tracy, 1988; Redman, 1990). Furthermore, the quantal size of EPSPs estimated in cat spinal motoneurones was relatively uniform, showing a small coefficient of variation (0·05; Jack *et al.* 1981). It was then hypothesized that the transmitter quanta might saturate the postsynaptic receptors in an all-or-none manner. Quantal release of the transmitter at central synapses has also been suggested by the recording of spontaneous miniature synaptic potentials (Katz & Miledi, 1963; Blankenship & Kuno, 1968; Brown, Wong & Prince, 1979; Takahashi, 1984), which are similar in characteristics to the miniature endplate potentials (Kojima & Takahashi, 1985). The amplitude of the miniature synaptic responses showed a relatively large coefficient of variation (0·33, Blankenship & Kuno, 1968; 0·19–0·30, Ropert, Miles & Korn, 1990; 0·42–0·55, Bekkers, Richerson & Stevens, 1990).

In the neuromuscular junction, a reduction in $[Ca^{2+}]_o$ diminished the endplate potentials, eventually to a level equivalent to the quantal size (Fatt & Katz, 1952; del Castillo & Katz, 1954). Synaptic transmission in central neurones is also highly dependent upon $[Ca^{2+}]_o$ (Kuno & Takahashi, 1986; Walmsley & Nicol, 1991). Therefore, evoked synaptic responses in central neurones may also be reduced to a level of quantal size by reducing the external Ca^{2+} concentration. Based on this assumption, the quantal size of IPSCs has been evaluated in the present study. These results are described in the Results section 'Minimal IPSCs'.

Inhibitory postsynaptic potentials (IPSPs) were first described in cat motoneurones by Coombs, Eccles & Fatt (1955). The IPSPs were originally assumed to be mediated by both potassium and chloride ions. Subsequently, the current responses induced by putative inhibitory transmitters glycine (Werman, Davidoff & Aprison, 1968) and GABA (Curtis & Johnston, 1974) have been shown to result from an increase in conductance exclusively to Cl^- (Borman, Hamill & Sakmann, 1987). Although Cl^- is undoubtedly the major ion contributing to the IPSCs, no evaluation has as yet been made for the relative contribution by potassium ions to IPSCs. This issue is studied in the Results section 'Ionic dependence of the IPSCs'.

All the studies were made by the whole-cell slice-patch method (Edwards, Konnerth, Sakmann & Takahashi, 1989). With this method, it was possible to record the IPSCs with high resolution under various internal and external ionic compositions.

A part of the present study has appeared in an abstract form (Takahashi, 1990*a*).

METHODS

Preparation

The experiments were carried out in lumbar spinal cord slices obtained from Wistar rats, 3–5 days old. Rats were rapidly and efficiently decapitated with scissors, and the lumbar spinal cord was quickly isolated. Slices 120 μm in thickness were prepared from the lumbar cord (L3–6) using a vibrating slicer as described previously (Takahashi, 1978, 1990*b*; Edwards *et al.* 1989). The slices were incubated at 37 °C for an hour and maintained thereafter by continuous perfusion at room temperature. Lactate (4 mM) was added to the incubation and maintenance solutions to improve the slice conditions (Schurr, West & Rigor, 1988).

Recording and solutions

Whole-cell recordings were made from motoneurones visually identified under Nomarski optics as described previously (Edwards *et al.* 1989; Takahashi, 1990*b*). The resistance of the patch pipette was 3–5 MΩ when filled with KCl or CsCl solution (solutions A and B, see below). The slices were continuously perfused with Krebs solution having the following ionic composition (mM): NaCl, 113; KCl, 3; NaH_2PO_4, 1; $NaHCO_3$, 25; glucose, 11; $CaCl_2$, 2; $MgCl_2$, 1. The pH of the solution was 7·4 when bubbled with O_2/CO_2 (95%/5%). When $[Cl^-]_o$ was reduced, NaCl was replaced by sodium gluconate and a 3 M-KCl–agar bridge was used as an indifferent electrode. When $[Ca^{2+}]_o$ was reduced, the osmolarity was balanced by sucrose.

The major ionic compositions of the pipette solutions (A–H) are as follows (mM): A, KCl (140); B, CsCl (140); C, NaCl (149); D, tetramethylammonium chloride (TMACl, 140); E, CsCl (55) and potassium gluconate (85); F, caesium acetate (122), CsCl (18) and KCl (2); G, potassium gluconate (129) and KCl (11); H, potassium gluconate (140). All internal solutions contained $MgCl_2$ (1 mM), EGTA (1 mM), HEPES (10 mM), NaCl (9 mM, but for C and F) and pH was adjusted with KOH (6 mM) to 7·4. In the experiments described in the Results section 'Minimal IPSCs', solution B was used. The Cl^- activities of internal (a^i_{Cl}) and external (a^o_{Cl}) solutions were calculated from the Cl^- concentrations, the activity coefficient for each Cl^- salt and the total ionic strength of the solutions (Robinson & Stokes, 1959). The E_{Cl} was calculated from the Nernst equation.

$$E_{Cl} = 59 \text{ mV } \log_{10}(a^i_{Cl}/a^o_{Cl}).$$

Because of the similar ionic strengths of external and internal solutions, the E_{Cl} values in the text were calculated from Cl^- concentrations instead of Cl^- activities, as a first approximation (error < 1 mV).

The liquid-junction potentials between the external and internal solutions were measured as described previously (Takahashi, 1990*b*). The values were +3 mV for solutions A and B, 0 mV for C, −2 mV for D, +6 mV for E, +7 mV for F and G and +11 mV for H. These values were corrected for the potential values in the text. A gigaohm seal (> 10 GΩ) was formed between a pipette and cell membrane before the patch was ruptured for whole-cell recording. Whole-cell currents were recorded with a patch clamp amplifier (EPC-7, List). The access resistance was less than 25 MΩ and routinely compensated by 50–70%. The input resistance of motoneurones measured with KCl internal solution near the resting potential was 0·3 GΩ on average (Takahashi, 1990*b*). The voltage error caused by the access resistance was not corrected. Data were stored on a PCM–videotape-recorder (DC–10 kHz), low-pass filtered at 1–3 kHz (−3 dB) and sampled at 2–20 kHz for the analysis by a computer (EPSON, PC-386).

The excitatory synaptic responses were blocked either by kynurenic acid (2 mM) or by 6-cyano-7-nitroquinoxaline-2,3-dione (CNQX, 2–10 μM). In the Results section 'Minimal IPSCs', GABAergic IPSCs were routinely abolished by bicuculline (10 μM) added to the perfusate. The IPSCs were evoked by a stimulating pipette filled with Krebs solution (resistance, 3–4 MΩ) placed gently on a nearby neurone (Fig. 1*B*). A voltage pulse (200 μs) was applied between the electrode and platinum wire in the bath.

Experiments were carried out mostly at room temperature (22–24 °C). When the temperature was raised, a perfusion line was warmed by a Peltier thermocouple, while the temperature was monitored by a thermister (tip diameter, 0·5 mm) positioned close to the slice. The perfusion speed was about 3·5 ml/min and the bath volume was 0·7 ml. The motoneurones were clamped at −75 mV unless otherwise indicated.

RESULTS

After the whole-cell configuration was attained in a motoneurone, extracellular stimuli were applied to a neighbouring neurone in the presence of glutamate receptor antagonists. The synaptic currents evoked by this procedure were largely abolished

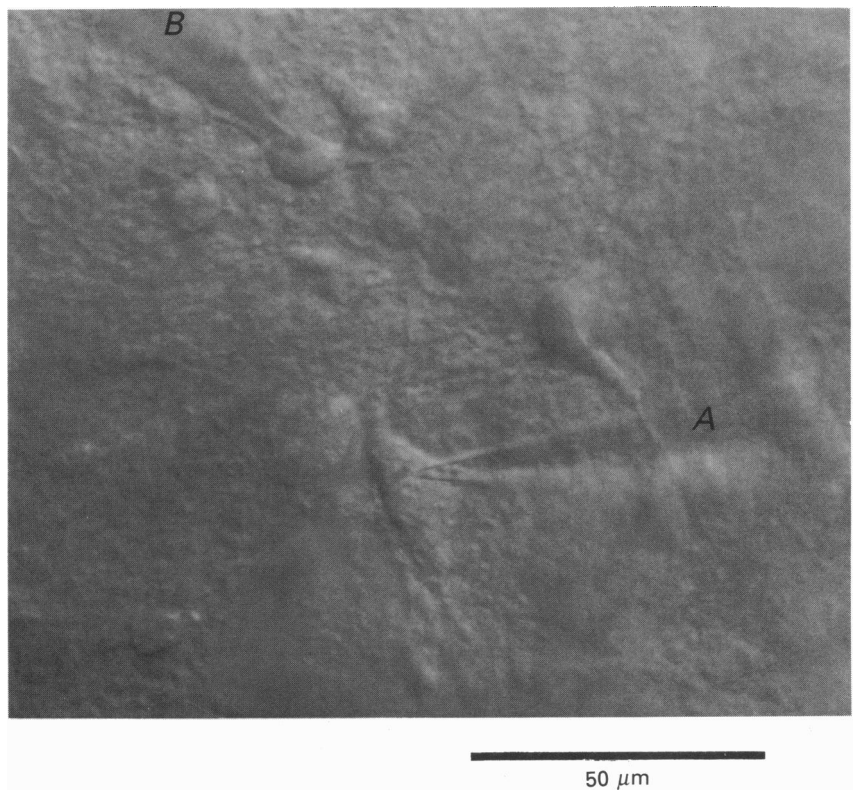

Fig. 1. The method of recording IPSCs in thin slices of rat spinal cord. *A*, a whole-cell patch electrode attached to a motoneurone. *B*, a Krebs solution-filled stimulating electrode placed on an internuncial neurone. Four-day-old rat.

by a low concentration of strychnine (0·5–2 μM, Edwards *et al.* 1989). Occasionally, however, a small component remained unabolished by strychnine. This component was completely blocked by addition of bicuculline (10 μM, T. Takahashi, A. Konnerth & B. Sakmann, unpublished observations). Therefore, the IPSCs recorded from neonatal rat spinal motoneurones appear to be mediated mainly by glycine and partly by GABA as previously reported for the cat spinal motoneurones (Cullheim & Kellerth, 1981). In the section 'Minimal IPSCs', IPSCs were recorded under CNQX and bicuculline to isolate the glycinergic IPSCs. In the section 'Ionic dependence of IPSCs', the perfusate did not contain bicuculline, thus possibly including both the GABAergic and glycinergic IPSCs.

Minimal IPSCs

Glycinergic IPSCs evoked monosynaptically by single inhibitory neurones

The IPSCs described in the following sections were recorded under bicuculline (10 μM) and CNQX (5 μM).

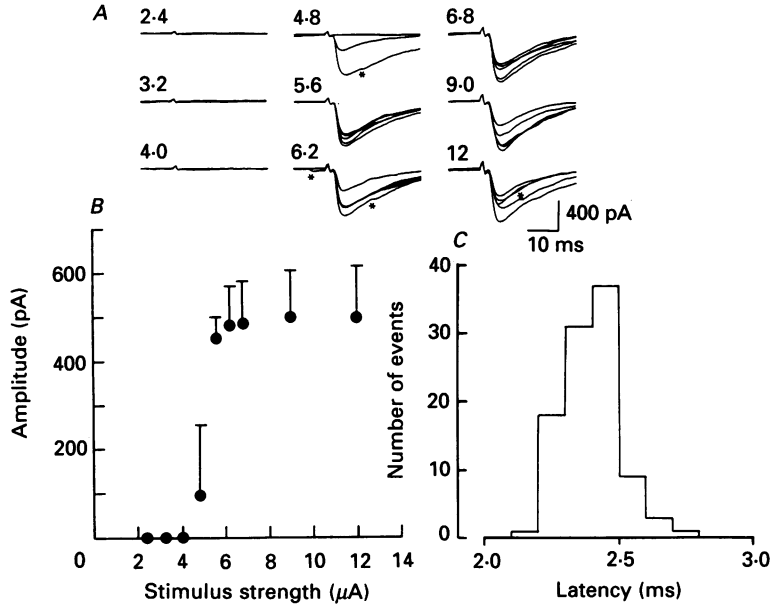

Fig. 2. Unitary characteristics of the IPSCs recorded from a motoneurone. *A* and *B*, all-or-none behaviour of IPSCs recorded from a motoneurone for gradually increased intensities of stimuli applied extracellularly to a nearby interneurone. Numbers in *A* and abscissa in *B* indicate stimulus strength (μA) measured from a virtual ground. Stimulus duration, 200 μs. Stimulus frequency, 0·5 Hz. Five consecutive records are superimposed in each frame in *A*. Spontaneous IPSCs are marked with asterisks. *B*, mean amplitude and S.D.s of IPSCs plotted against stimulus strength. *C*, latency histogram of the IPSCs. Data were sampled at 2 kHz in *A* and 10 kHz for *C*.

The unitary IPSCs. IPSCs were evoked by stimulating single internuncial neurones. The unitary nature of the IPSCs was examined, using the following criteria. When the stimulus intensity was gradually increased, the IPSCs abruptly appeared with frequent failures (three out of five trials, Fig. 2*A*, top traces in the middle column). When the stimulus strength was further increased, the failure became infrequent (Fig. 2*A*, no failure in five trials above 5·6 μA). The amplitudes of individual IPSCs fluctuated but their mean value was nearly constant for a certain range of stimulus intensity above the threshold (Fig. 2*B*). On occasions, the mean amplitude of IPSCs increased by increasing the stimulus strength implying recruitment of additional interneurones by current spread. These IPSCs were excluded from the analysis. To avoid the possible failures due to insufficient stimulus strength, the IPSCs were evoked at an intensity of about 1·5 times higher than the threshold. The possibility of direct activation of presynaptic boutons by current spread was excluded because of abolishment of IPSCs by TTX application (0·3 μM, see below).

The unitary nature of the IPSCs was also supported by the narrowly ranged latency. The latency measured from the stimulus artifact to the onset of IPSCs may include the axonal conduction time and the synaptic delay. The latency histogram (Fig. 2*C*) was unimodal with a fluctuation range of less than 1 ms.

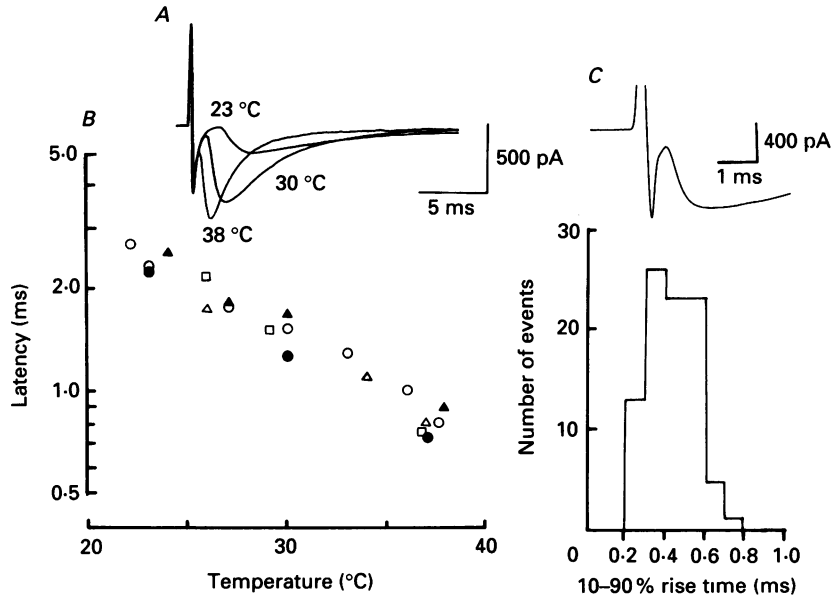

Fig. 3. *A*, IPSCs recorded from a motoneurone at different temperatures (23, 30 and 38 °C). Averaged records are superimposed. *B*, latency of IPSCs at different temperatures on semilogarithmic plot. Different symbols in this and following figures (Figs 4 and 6) indicate the data derived from different motoneurones. *C*, rise time (10–90 %) distribution of individual IPSCs recorded from a motoneurone at 37 °C with their averaged record in inset.

The monosynaptic nature of the IPSCs. Since glutamate receptors were blocked by CNQX, the chance of evoking polysynaptic responses must be small. The monosynaptic nature of the IPSCs was confirmed by measuring the latency at 37 °C. At room temperature, the latency of the IPSCs ranged between 2 and 3 ms (Fig. 3*B*). When the temperature was raised, the latency became shorter (Fig. 3*A* and *B*), and both the rise and decay times of IPSCs were reduced (Fig. 3*A*). Shortening of the rise and decay times at higher temperatures suggests that the IPSCs are not seriously distorted by the cable properties. At 37 °C, the mean latency was $0{\cdot}81 \pm 0{\cdot}07$ ms ($\pm$S.D., five cells). In cat spinal cord, the minimum latency for the disynaptic responses was estimated to be 1·0 ms (Kuno & Weakly, 1972). Therefore, the observed latency of IPSCs meets the criteria for a monosynaptic response. An additional support for the monosynaptic activation was the resistance to fatigue during repetitive stimulation. At a stimulus frequency of 50 Hz, the magnitude of IPSCs was reduced to 49 ± 27 % of control (seven cells). Between 0·2 and 20 Hz, no appreciable fatigue was observed. In the following experiments, IPSCs were evoked at 2 Hz.

Figure 3*C* illustrates the rise time (10–90 %) distribution of IPSCs recorded from a motoneurone at 37 °C. In this motoneurone, the rise time was in the range of 0·2–0·8 ms with a mean of 0·43 ms. The average rise time of IPSCs recorded from five motoneurones was 0·42 ± 0·08 ms which is comparable to the mean rise time

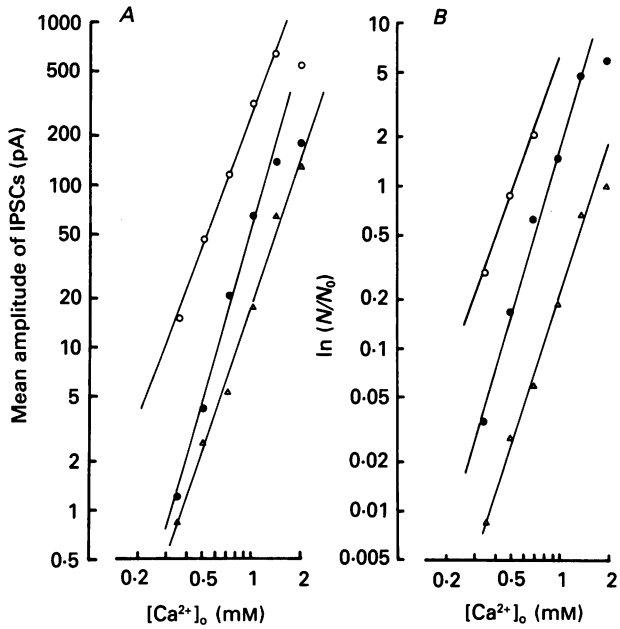

Fig. 4. *A*, the relationship between the mean amplitude of IPSCs and $[Ca^{2+}]_o$. *B*, $\log_e (N/N_0)$ plotted against $[Ca^{2+}]_o$. Both *A* and *B*, double logarithmic co-ordinates. The fitting lines were drawn by the least-squares method in this figure and Figs 9*B* and 12*B*. The values at 2 mM $[Ca^{2+}]_o$ were skipped from fitting in this figure. Each data point derived from 300–1000 trials in three motoneurones.

(10–90 %) reported for unitary IPSCs in cat motoneurones (0·40 ms; Stuart & Redman, 1990). On the other hand, the decay time course of IPSCs recorded at 37 °C was much slower than those reported in cat motoneurones (Araki & Terzuolo, 1962; Stuart & Redman, 1990). The half-decay time of IPSCs was 2·4 ms on average (± 0·83 ms, five cells), which is about three times slower than the mean decay time constant of IPSCs reported in cat motoneurones (Stuart & Redman, 1990). By analogy to the neuromuscular junction (Sakmann & Brenner, 1978), the slow decay time observed for the IPSCs may reflect the properties of the inhibitory receptor channels at early developmental stages.

Effects of $[Ca^{2+}]_o$ *reduction on the IPSCs*

Failures and the mean amplitude of IPSCs. When $[Ca^{2+}]_o$ was gradually reduced, leaving $[Mg^{2+}]_o$ at 1 mM, the rate of failures to trials (N_0/N) markedly increased. For example this rate observed in a motoneurone was 0·42–0·65 in normal $[Ca^{2+}]_o$ during 30 min (sampled every 30 s). Within 2 min after reducing $[Ca^{2+}]_o$ to 0·7 mM, N_0/N increased to 0·88–0·96. The rate recovered to the control level within 1 min after

raising the Ca^{2+} concentration to the normal level. The inverse relationship between the rate of failures and $[Ca^{2+}]_o$ concentration is illustrated in Fig. 4*B*. The relationship between $\ln N/N_0$ (the reciprocal of the rate of failures) and $[Ca^{2+}]_o$ could be fitted to straight lines on double logarithmic co-ordinates between 1·4 and 0·35 mM $[Ca^{2+}]_o$.

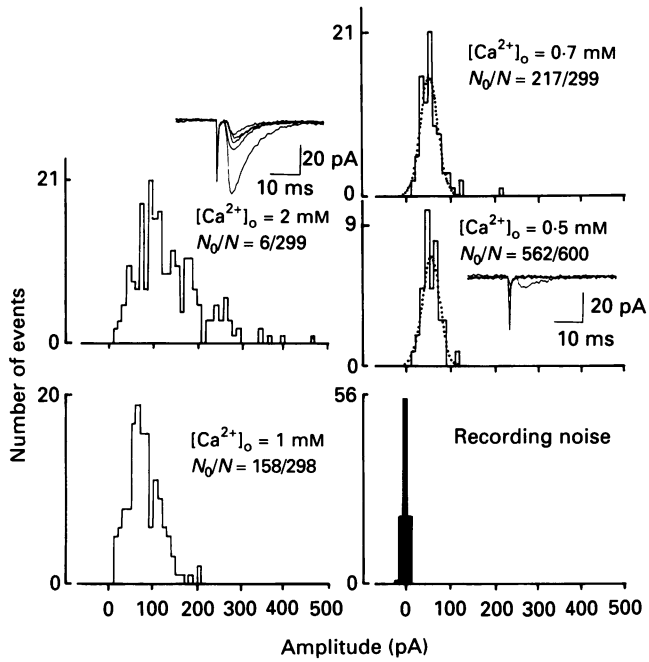

Fig. 5. The amplitude histograms of IPSCs in a motoneurone at various $[Ca^{2+}]_o$ (indicated together with N_0/N values in each panel). Five consecutive records were superimposed in insets at 2 mM and 0·5 mM $[Ca^{2+}]_o$. Filled column in the right bottom histogram represents background noise sampled from records 10–20 ms before stimulation in 0·5 mM $[Ca^{2+}]_o$. The dotted line represents a Gaussian curve in this figure and Fig. 7*B*. The peak amplitudes ± S.D.s were 50 ± 21 pA in 0·7 mM $[Ca^{2+}]_o$ and 52 ± 21 pA in 0·5 mM $[Ca^{2+}]_o$.

In 2 mM $[Ca^{2+}]_o$, the unitary IPSCs had a mean amplitude of 232 ± 153 pA at −75 mV (twenty cells) corresponding to 2·9 ± 1·9 nS (E_{IPSC} = 4 mV with internal solution B, see Fig. 10*B*), which was about one-third of that reported for the unitary IPSCs (Stuart & Redman, 1990) and three-fifths of the unitary EPSCs (Finkel & Redman, 1983) in cat motoneurones. When $[Ca^{2+}]_o$ was reduced, the mean amplitude of IPSCs decreased (Fig. 4*A*) with an increase in failures (Fig. 4*B*). The relationship between the mean amplitude and $[Ca^{2+}]_o$ was highly non-linear. Between 0·35 and 1·4 mM $[Ca^{2+}]_o$, the relation was fitted by a straight line on double logarithmic co-ordinates with a slope of 3·1 ± 0·67 (eight cells). This value is comparable to that reported for the amphibian (3·8, Dodge & Rahamimoff, 1967) and mammalian (3·3–3·4, Cull-Candy, Miledi, Trautmann & Uchitel, 1980) neuromuscular junctions. Between 1·4 and 2·0 mM $[Ca^{2+}]_o$, the effects of $[Ca^{2+}]_o$ tended to saturate (Fig. 4*A*, ● and ○; 4*B*, ● and △) similarly to those reported for the endplate potentials (Dodge & Rahamimoff, 1967; Cull-Candy *et al.* 1980).

As in neuromuscular junctions (Dodge & Rahamimoff, 1967) and excitatory synapses on neonatal rat motoneurones (Kuno & Takahashi, 1986), $[Ca^{2+}]_o$ and $[Mg^{2+}]_o$ showed opposite effects on IPSCs. When $[Ca^{2+}]_o$ was reduced by replacement of $[Mg^{2+}]_o$, the mean amplitude of IPSCs decreased much more steeply with a double logarithmic slope of $5{\cdot}9 \pm 1{\cdot}6$ (three cells, 0·5–1·4 mM $[Ca^{2+}]_o$).

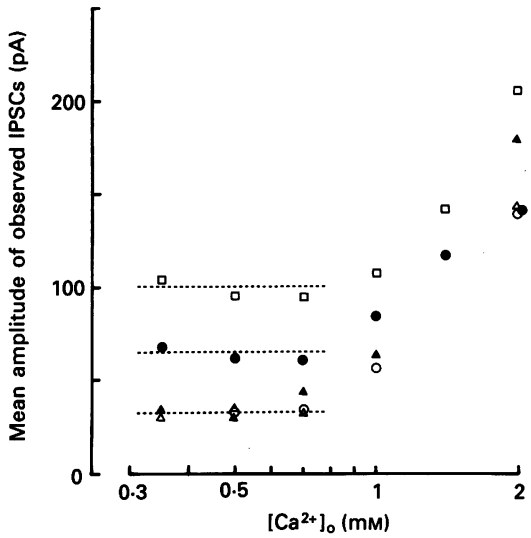

Fig. 6. The mean amplitude of observed IPSCs in five motoneurones plotted against $[Ca^{2+}]_o$ (0·35–2 mM). Failures were not included in amplitude calculations (cf. Fig. 4*A*).

The minimal IPSCs. Figure 5 illustrates the amplitude histograms of IPSCs observed in a motoneurone in different $[Ca^{2+}]_o$. As $[Ca^{2+}]_o$ was reduced, the occurrence of large IPSCs became less frequent and the range of amplitude fluctuation decreased. At 0·7 and 0·5 mM $[Ca^{2+}]_o$, the amplitude distribution of IPSCs was similar, each being fitted by a Gaussian curve with a nearly identical peak amplitude and S.D. In five out of eleven motoneurones, the amplitude distribution of IPSCs examined at 0·5 mM $[Ca^{2+}]_o$ was described by a Gaussian curve, whereas the distribution showed clear skewness towards the large amplitude in six other motoneurones.

Figure 6 illustrates the relationship between the mean amplitude of observed IPSCs (excluding failures) and $[Ca^{2+}]_o$ in five motoneurones (different symbols). When $[Ca^{2+}]_o$ was reduced, the mean amplitude clearly decreased between 2·0 and 1·0 mM $[Ca^{2+}]_o$ but reached a steady minimum level below 0·7 mM $[Ca^{2+}]_o$. This is in contrast with the steep dependence of the rate of failures on $[Ca^{2+}]_o$ observed between 0·7 and 0·35 mM (Fig. 4*B*). These results suggest that stimulation of a single neurone in 0·35–0·7 mM $[Ca^{2+}]_o$ fails to release the transmitter or releases only one quantum of the transmitter.

As the number of failures increased in low $[Ca^{2+}]_o$, some spontaneous IPSCs might be included as evoked responses. This probability was estimated from the mean frequency of spontaneous events, the number of stimuli and the variability in

latency. For example, the chance was 2·3% in 0·7 mM $[Ca^{2+}]_o$ and 10% in 0·5 mM $[Ca^{2+}]_o$ for the IPSCs illustrated in Fig. 5 (the mean frequency of spontaneous events, 6·5 Hz; allowance for latency fluctuation, 1 ms). In another motoneurone, the probability was 0·9 and 2·3%, respectively, in 0·7 and 0·5 mM $[Ca^{2+}]_o$. Apparently,

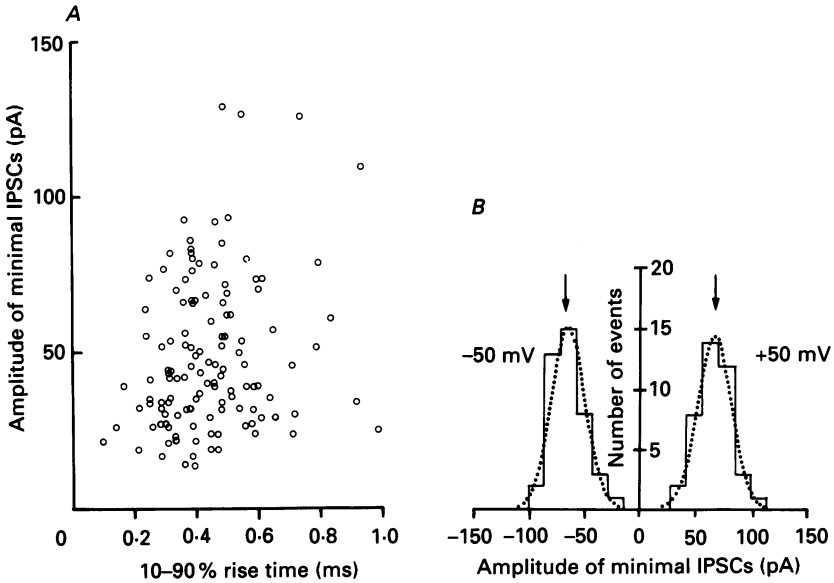

Fig. 7. *A*, the relationship between amplitude and rise time (10–90%) of individual minimal IPSCs recorded in a motoneurone in 0·5 mM $[Ca^{2+}]_o$. Data sampled at 20 kHz. *B*, amplitude histogram of minimal IPSCs recorded in 0·5 mM $[Ca^{2+}]_o$ from another motoneurone at the holding potentials of −50 mV (left) and +50 mV (right). Positive and negative sign in abscissae each indicates the outward and inward current amplitude in this figure. Peak amplitudes (arrows) ±S.D. of the Gaussian curves were −60·7±15·9 pA at −50 mV and 62·8±16·4 pA at +50 mV.

the majority of the minimal IPSCs observed in low $[Ca^{2+}]_o$ must be evoked by quantal emission of the transmitter at the synapses formed by the neurone stimulated. The mean size of the minimal IPSCs was 51·9±22·2 pA (eight cells), corresponding to 657±281 pS.

The IPSCs observed in two motoneurones behaved differently from those observed in eleven other motoneurones. In these cases, the number of failures increased on reducing $[Ca^{2+}]_o$, but small IPSCs, instead of large IPSCs, disappeared. Thus, a reduction of $[Ca^{2+}]_o$ resulted in an increase in the mean amplitude of observed IPSCs. The meaning of these results is not clear.

Variability in the minimal IPSCs. The minimal IPSCs evoked in low $[Ca^{2+}]_o$ had a variance at least 4 times larger than that measured for the recording noise (Fig. 5, filled column). The coefficient of variation (C.V. = S.D./mean) for the minimal IPSCs measured at 0·5 mM $[Ca^{2+}]_o$ was 0·50±0·13 (eight cells). This variability might be due to various degrees of electrotonic attenuation of the IPSCs evoked at different release sites. To test this possibility, the relationship between the rise time (10–90%) and amplitude of individual minimal IPSCs was examined in a motoneurone. As shown in Fig. 7*A*, no correlation was observed between the two parameters. This suggests a genuine variability in the size of minimal IPSCs.

If the space voltage clamp was inadequate, the apparent E_{IPSC} would deviate from the real value. This was not the case, and the E_{IPSC} consistently agreed with the E_{Cl} predicted from the various ionic compositions used in different experiments (Fig. 10). To examine the possible inadequate voltage control further, the amplitude

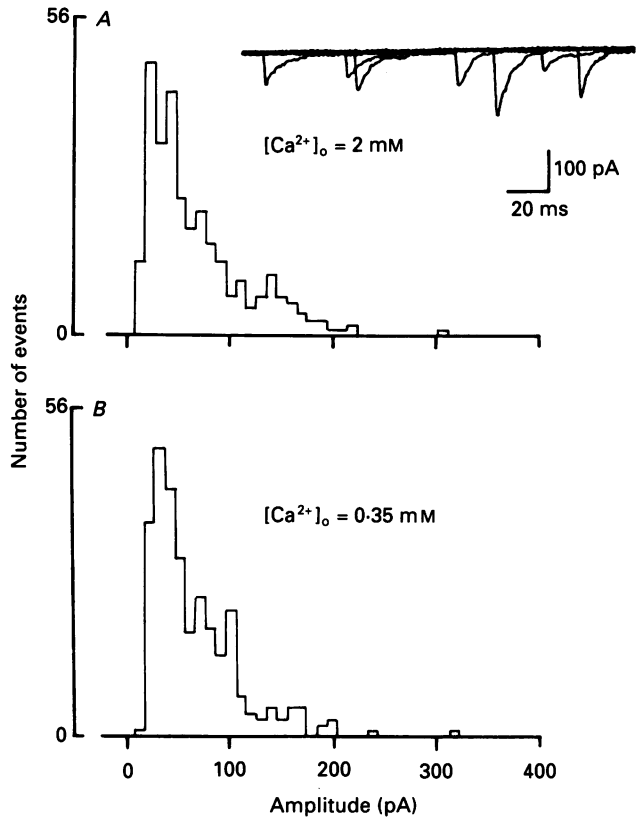

Fig. 8. Spontaneous miniature IPSCs recorded from a motoneurone under TTX (0·3 μM). Amplitude histograms in 2 mM (*A*) and 0·35 mM (*B*) $[Ca^{2+}]_o$. Five traces are superimposed in inset in *A*. The mean frequency was 3·8 Hz in *A* and 2·1 Hz in *B*.

distribution of IPSCs was obtained at two different holding potentials. Figure 7*B* illustrates the amplitude distributions of minimal IPSCs evoked in a motoneurone in 0·5 mM $[Ca^{2+}]_o$ at -50 and $+50$ mV. The minimal IPSCs were recorded as inward currents at -50 mV and outward currents at $+50$ mV. The two amplitude histograms were nearly symmetrical, having virtually the same coefficient of variation (see legend).

Miniature IPSCs

When TTX (0·3 μM) was added to the perfusate, the evoked IPSCs were completely abolished. TTX in this concentration suppressed the action potential or voltage-gated sodium currents in motoneurones (Takahashi, 1990*b*). Similarly, replacement of external Ca^{2+} with Mg^{2+} or Mn^{2+} or mere addition of Cd^{2+} (50 μM)

reversibly abolished the IPSCs, suggesting that the inhibitory transmission is mediated by the high-voltage-activated Ca^{2+} channels (Carbone & Lux, 1987; Fox, Nowycky & Tsien, 1987; Berger & Takahashi, 1990).

Spontaneous miniature IPSCs were recorded after synaptic transmission was blocked by TTX (Fig. 8*A*, inset), Mn^{2+} or Cd^{2+} (not shown). They occurred at a mean

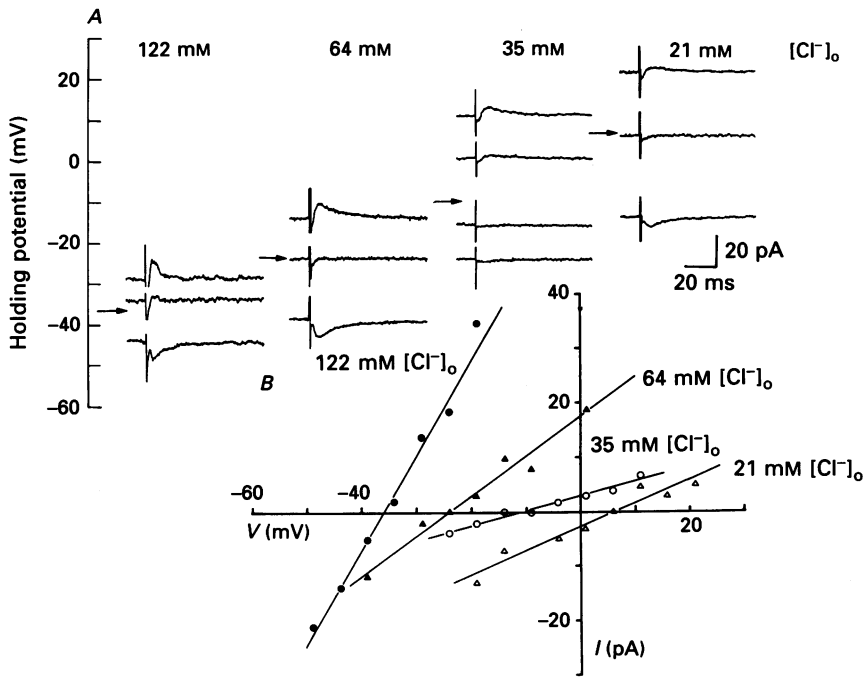

Fig. 9. IPSCs recorded from a motoneurone under various $[Cl^-]_o$. Internal Cl^- concentration was 22 mM (solution F, Methods). Averaged records of IPSCs (*A*) and their *I–V* relations (*B*). $[Cl^-]_o$ was reduced by replacement with gluconate. Arrows in *A* indicate the reversal potentials of IPSCs at different $[Cl^-]_o$.

frequency of 0·4–14 Hz (fifteen cells) and were reversibly abolished by strychnine (0·5 μM, not shown). Their amplitude histogram (Fig. 8*A*) showed various degrees of skewness in different motoneurones. The mean amplitude of miniature IPSCs was 58·4 ± 22 pA (fifteen cells) corresponding to 739 ± 278 pS and their c.v. was 0·66 ± 0·14 (fifteen cells). Thus, the miniature IPSCs were similar in magnitude to the minimal evoked IPSCs ($P > 0·1$, *t* test). However, the c.v. was significantly larger in miniature IPSCs than that of minimal IPSCs ($P < 0·05$). Apparently, the large c.v. is attributed to the skewness of the amplitude distribution of miniature IPSCs.

When $[Ca^{2+}]_o$ was reduced from 2 to 0·35 mM, the mean frequency of miniature IPSCs declined on average to 49% of control (five cells), whereas their mean amplitude remained unchanged (105 ± 15%, eight cells; Fig. 8*B*; see also Kojima & Takahashi, 1985). The miniature IPSCs also occurred at similar low frequencies in a solution containing Cd^{2+} (50 μM). In mammalian neuromuscular junctions (Boyd & Martin, 1956; Hubbard, Jones & Landau, 1968) and inhibitory synapses in

motoneurones (Kojima & Takahashi, 1985), the frequency of miniature synaptic responses was shown to be dependent upon $[Ca^{2+}]_o$.

Ionic dependence of the IPSCs

The reversal potential of IPSCs under various concentrations of external and internal Cl^-

IPSCs were recorded in the presence of glutamate receptor antagonists from a motoneurone under various $[Cl^-]_o$. The mean amplitude of IPSCs was linearly related

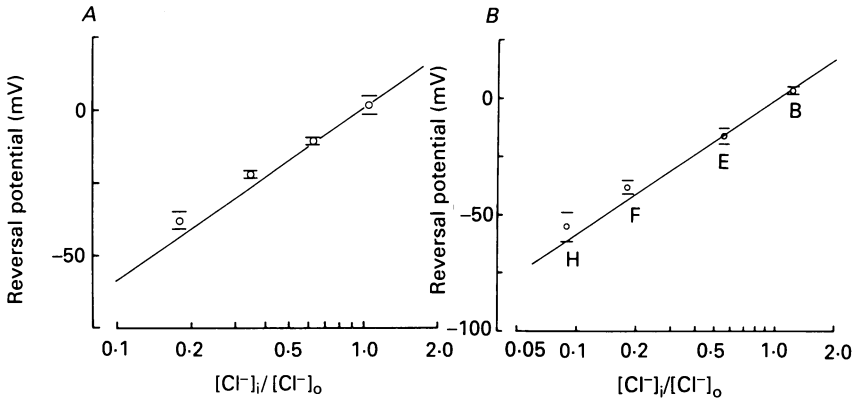

Fig. 10. The reversal potential of IPSCs (E_{IPSC}) plotted against the logarithmic ratio of internal and external Cl^- concentrations ($[Cl^-]_i/[Cl^-]_o$). *A*, at various $[Cl^-]_o$ and fixed $[Cl^-]_i$ (22 mM, solution F). *B*, at various $[Cl^-]_i$ (151, 66, 22, 11 mM, solutions B, E, F, H as indicated) and fixed $[Cl^-]_o$ (122 mM, Krebs solution). Mean values of E_{IPSC} and S.D.s are indicated by symbols and bars in this and following figures (Figs 11 and 12). Each data point derived from five cells in *A* and five to six cells in *B*. In *A* and *B*, a straight line was drawn according to the Nernst equation for E_{Cl}.

to the holding potential and the E_{IPSC} was estimated by interpolating their amplitudes at different potentials (Fig. 9*B*). With 22 mM $[Cl^-]_i$ (solution F, Methods) and 122 mM $[Cl^-]_o$ (Krebs solution), IPSCs reversed polarity at around −35 mV (Fig. 9*A*, left column; Fig. 9*B*, ●). As $[Cl^-]_o$ was reduced, the E_{IPSC} (arrows in Fig. 9*A*) shifted in a positive direction.

The E_{IPSC} estimated under various $[Cl^-]_o$ were plotted against the ratio of $[Cl^-]_i/[Cl^-]_o$ on semilogarithmic co-ordinates (Fig. 10*A*). The IPSCs were also recorded with various $[Cl^-]_i$. When K^+ in internal solution (A) was replaced by Cs^+ (B), Na^+ (C) or TMA (D), the E_{IPSC} was not significantly altered: 7·9 ± 7·5 mV (A, six cells); 4·1 ± 1·2 mV (B, seven cells); 2·4 ± 1·2 mV (C, five cells); 3·8 ± 1·4 mV (D, five cells). The E_{IPSC} values obtained with various $[Cl^-]_i$ (B, E, F, H) are illustrated in Fig. 10*B*. Thus, the E_{IPSC} under various $[Cl^-]_o$ and $[Cl^-]_i$ agreed approximately with the E_{Cl} calculated from the Nernst equation (straight lines in *A* and *B*).

E_{IPSC} under various $[K^+]_o$ and $[K^+]_i$

The possible contribution of K^+ permeability to IPSCs has been suggested by Coombs *et al.* in cat spinal motoneurones (1955) and more recently by Mercuri, Calabresi & Bernardi (1988) in mesencephalic neurones. This possibility was tested

by measuring E_{IPSC} under various $[K^+]_o$ and $[K^+]_i$ (Fig. 11). When $[K^+]_o$ was reduced 30-fold from 3 to 0·1 mM while maintaining $[K^+]_i$ at 146 mM (solution A) the E_{IPSC} showed no significant change (Fig. 11*A*; Fig. 11, middle and left points). The E_{IPSC} estimated with low $[K^+]_i$ (6 mM, solution D; Fig. 11*B*, right point) was also similar

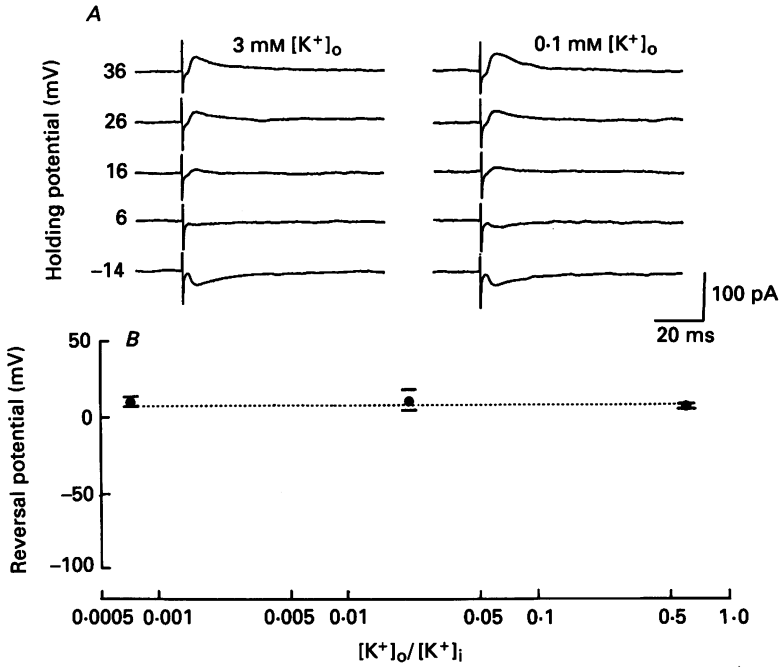

Fig. 11. *A*, IPSCs recorded from a motoneurone at various holding potentials in 3 and 0·1 mM $[K^+]_o$. $[K^+]_i$, 146 mM (solution A). *B*, the E_{IPSC} plotted against log $[K^+]_o/[K^+]_i$. The left and middle data points derived from the experiments as shown in *A*. The right data point was from the experiments with 6 mM $[K^+]_i$ (solution D) and 3 mM $[K^+]_o$ (Krebs solution). Each data point derived from three to four motoneurones.

to that estimated with normal $[K^+]_i$ (solution A). Thus, the E_{IPSC} was nearly the same for a 730-fold change of $[K^+]_o/[K^+]_i$.

Relative permeability for Cl^- and K^+

An attempt was made to determine the upper limit of the K^+/Cl^- permeability ratio (P_K/P_{Cl}, Fig. 12) for the IPSCs. Cs^+ was omitted from the internal solution to exclude the possibility that internal Cs^+ may interfere with P_K (Mercuri *et al.* 1988). When $[Cl^-]_o$ was reduced from 122 to 21 mM with 22 mM $[Cl^-]_i$, E_{IPSC} shifted by 43·5±4·5 mV (six cells, ● in Fig. 12*C*). The magnitude of the shift coincided approximately with that predicted from the E_{Cl} (45·1 mV, Fig. 12*C*, top curve).

If IPSCs were carried by both Cl^- and K^+, the E_{IPSC} could be estimated by the constant-field equation (Goldman, 1943; Hodgkin & Katz, 1949):

$$E_r = (RT/F)\ln(P_{Cl}[Cl^-]_i + P_K[K^+]_o)/(P_{Cl}[Cl^-]_o + P_K[K^+]_i).$$

The curves were drawn for various P_K/P_{Cl} (0–0·20) in Fig. 12*C*. From the data points on these curves, the upper limit for P_K/P_{Cl} can be estimated to be 0·05.

In cat motoneurones, the inhibitory receptor channel has been reported to be permeable to HCO_3^- (Araki, Ito & Oscarsson, 1961; Ito, Kostyuk & Oshima, 1962). When HCO_3^- was removed from the external solution maintaining its pH with HEPEs (10 mM), the E_{IPSC} shifted from $4{\cdot}1 \pm 1{\cdot}5$ to $8{\cdot}0 \pm 1{\cdot}8$ mV (four cells, $P < 0{\cdot}05$, internal solution B). Thus, HCO_3^- must be involved partly in the IPSCs.

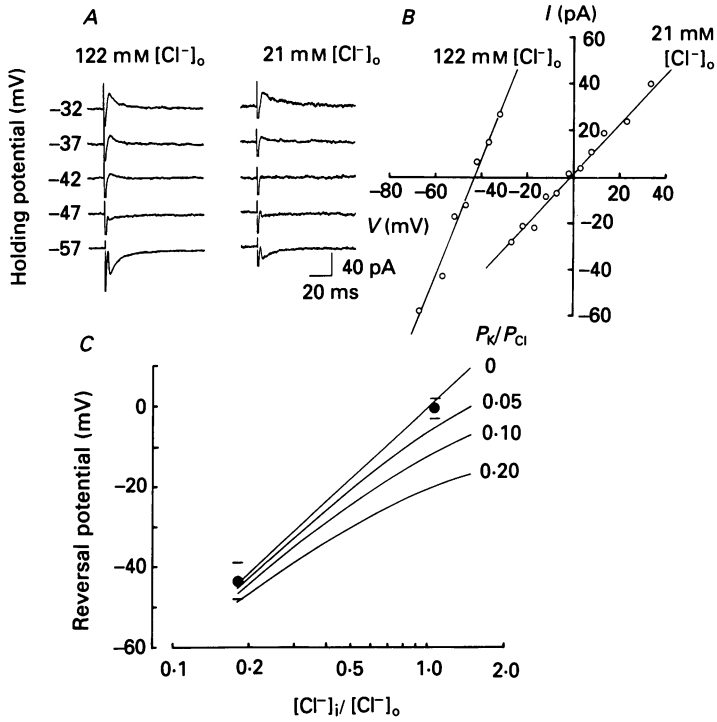

Fig. 12. Estimation of the K^+/Cl^- permeability ratio, P_K/P_{Cl}. *A*, the IPSCs recorded in a motoneurone with 22 mM $[Cl^-]_i$ (solution G) in 122 mM $[Cl^-]_o$ and in 21 mM $[Cl^-]_o$. *B*, the *I–V* relation of the IPSCs. *C*, the mean E_{IPSC} (six cells) measured at two different $[Cl^-]_i/[Cl^-]_o$. The curves were drawn according to the constant-field equation with various P_K/P_{Cl} values as indicated.

DISCUSSION

Whole-cell recording of IPSCs in motoneurones

In the present study, whole-cell recordings of IPSCs were made from motoneurones visually identified in thin slices of neonatal rat spinal cord. One of the advantages of the whole-cell recording is that the extracellular ionic composition can be freely changed, while the intracellular ionic composition is maintained by the pipette solution (Pusch & Neher, 1988). Another advantage is a high resolution of the signal (Edwards *et al.* 1989).

Minimal evoked IPSCs

The principal aim of the present study was to isolate the quantal IPSCs. This was achieved by reducing $[Ca^{2+}]_o$. When $[Ca^{2+}]_o$ was decreased, the amplitude of individual IPSCs decreased and eventually reached a minimum level. Most of the

evoked IPSCs showed the minimum size at low $[Ca^{2+}]_o$ below 0·7 mM at which the number of failures still continued to increase. The mean amplitude of minimal IPSCs was comparable to that of miniature IPSCs (see also, Kojima & Takahashi, 1985). Therefore, it is suggested that the minimal IPSCs represent the IPSCs evoked by a quantal packet of transmitter. In hippocampal GABAergic synapses, the IPSCs evoked in 0·5 mM-Ca^{2+} and 2·5 mM-Mg^{2+} also showed an amplitude similar to the peak interval of the amplitude histogram in normal solution (Edwards, Konnerth & Sakmann, 1990).

Amplitude of the minimal IPSCs

The minimal IPSCs had a mean conductance of 657 pS which was comparable to that of the miniature IPSCs. This was about one-tenth of the quantal conductance change estimated in cat motoneurones (5–8 nS, Kuno & Weakly, 1972). The unitary IPSCs had a mean conductance of 2·9 nS. This implies that the mean quantal content of the inhibitory synapse is, on average, 4·4 which agrees with the previous estimate in cat spinal motoneurones (2–5, Kuno & Weakly, 1972).

The magnitude of the unitary IPSCs was one-third of that reported in cat spinal motoneurones (9·1 nS, Stuart & Redman, 1990). Since the main conductance state of the synaptic glycine receptor channel is 43 pS (Takahashi & Momiyama, 1991), the average number of channels activated for a minimal IPSC is estimated to be fifteen. This agrees reasonably well with the number of synaptic channels directly observed in the decay phase of glycinergic IPSCs in rat dorsal horn neurones (Takahashi & Momiyama, 1991). A similar figure has been reported for GABA-mediated IPSCs in hippocampal neurones from the quantal size estimated from the peak interval of the amplitude histogram of IPSCs (six to thirty channels, Edwards *et al.* 1990) or from the mean amplitude of miniature IPSCs (< sixty, Cull-Candy & Usowicz, 1989; twelve to twenty, Ropert *et al.* 1990). These numbers are about 100 times smaller than those estimated for the quantal size of glycinergic IPSCs in lamprey spinal cord (1500, Gold & Martin, 1983), goldfish Mauthner cells (1400, Korn, Burnod & Faber, 1987) as well as for the miniature endplate potentials in amphibian neuromuscular junctions (1000, Katz & Miledi, 1972; 1700, Anderson & Stevens, 1973).

Variability in the amplitude of minimal IPSCs

The minimal IPSCs evoked in a motoneurone had a relatively large variation with a mean c.v. of 0·50, compared with the noise level. This variation is much larger than those reported for the quantal size estimated with deconvolution analysis in the excitatory synapses of cat motoneurones (c.v., 0·05, Jack *et al.* 1981) and that statistically estimated in inhibitory synapse of lamprey (0·15, Gold & Martin, 1983) and goldfish neurones (0·11, Korn *et al.* 1987). If the amplitude dispersion of minimal evoked IPSCs were due to various degrees of their electrotonic attenuation, the larger response should have a faster rise time (del Castillo & Katz, 1956). The rise time–amplitude relation histogram indicated that this is not the case. Furthermore, the amplitude of minimal IPSCs changed with changes in the holding potential. Thus, the dispersion of the minimal IPSCs appears to reflect the non-uniform quantal size (see also, Ropert *et al.* 1990). A similarly large variation in quantal size has been reported for the miniature excitatory synaptic currents locally evoked with

hypertonic solution (c.v., 0·42–0·55, Bekkers *et al.* 1990) and for the statistically estimated quantal size (c.v., 0·39, Yamamoto, Higashima, Sawada & Kamiya, 1991) in hippocampal neurones.

In the neuromuscular junction, the postsynaptic receptors are not saturated by a quantal transmitter action (Hartzell, Kuffler & Yoshikami, 1975). Therefore, the quantal size is determined by the amount of transmitter in a quantal packet. However, in excitatory synapses of cat spinal cord, based on the small c.v. of quantal size (0·05), Jack *et al.* (1981) have postulated that the quantum may saturate the postsynaptic receptors in an all-or-none manner, the quantal size being determined by the receptor density. This hypothesis was supported in other synapses (Korn *et al.* 1987; Stuart & Redman, 1990; Edwards *et al.* 1990). Clearly, the discrepancy on the variability of quantal size requires further investigations. The present study also showed that the amplitude of minimal IPSCs has a normal distribution in 50% of motoneurones examined, whereas the amplitude of miniature IPSCs invariably showed skewness. These results remain a puzzle.

Ionic dependence of IPSCs

In the present study, the ionic basis for the IPSCs was also examined. Under the whole-cell recording condition, intracellular ionic composition is quickly equilibrated with the pipette solution (Pusch & Neher, 1988). This excludes the possibility of intracellular ionic redistribution by diffusion (Hodgkin & Horowicz, 1959) or the disturbance of active ion co-transport mechanisms (Inagaki, Oda, Kondo & Kusumi, 1987; Alvarez-Leefmans, 1990). The IPSCs reversed in polarity near the E_{Cl} under various external and internal Cl^- concentrations. In contrast, a large change in the potassium concentration gradient across the membrane did not affect the E_{IPSC}. The upper limit of P_K/P_{Cl} was estimated to be 0·05. Thus, it is concluded that the IPSCs in neonatal rat motoneurones are carried almost exclusively by Cl^-.

I am grateful to Drs Motoy Kuno and Stuart G. Cull-Candy for their critical reading of the manuscript. This study was supported by Grants-in-Aid for Scientific Research from the Ministry of Education, Science and Culture of Japan (Nos. 01480124 and 01659002).

REFERENCES

ALVAREZ-LEEFMANS, F. J., GAMINÕ, S. M., GIRALDEZ, F. & NOGUREÒN, I. (1988). Intracellular chloride regulation in amphibian dorsal root ganglion neurones studied with ion-selective microelectrodes. *Journal of Physiology* **406**, 225–246.

ANDERSON, C. R. & STEVENS, C. F. (1973). Voltage clamp analysis of acetylcholine produced end-plate current fluctuations at frog neuromuscular junction. *Journal of Physiology* **235**, 655–691.

ARAKI, T. & TERZUOLO, C. A. (1962). Membrane currents in spinal motoneurons associated with the action potential and synaptic activity. *Journal of Neurophysiology* **25**, 772–789.

ARAKI, T., ITO, M. & OSCARSSON, O. (1961). Anion permeability of the synaptic and non-synaptic motoneurone membrane. *Journal of Physiology* **159**, 410–435.

BEKKERS, J. M., RICHERSON, G. B. & STEVENS, C. F. (1990). Origin of variability in quantal size in cultured hippocampal neurons and hippocampal slices. *Proceedings of the National Academy of Sciences of the USA* **87**, 5359–5362.

BERGER, A. J. & TAKAHASHI, T. (1990). Serotonin enhances a low-voltage-activated calcium current in rat spinal motoneurons. *Journal of Neuroscience* **10**, 1922–1928.

BLANKENSHIP, J. E. & KUNO, M. (1968). Analysis of spontaneous subthreshold activity in spinal motoneurons of the cat. *Journal of Neurophysiology* **31**, 195–209.

BORMANN, J., HAMILL, O. P. & SAKMANN, B. (1987). Mechanism of anion permeation through

channels gated by glycine and γ-aminobutyric acid in mouse culture spinal neurones. *Journal of Physiology* **385**, 243–286.

BOYD, I. A. & MARTIN, A. R. (1956). Spontaneous subthreshold activity at mammalian neuromuscular junctions. *Journal of Physiology* **132**, 61–73.

BROWN, T. H., WONG, R. K. S. & PRINCE, D. A. (1979). Spontaneous miniature synaptic potentials in hippocampal neurons. *Brain Research* **177**, 194–199.

CARBONE, E. & LUX, H. D. (1987). Kinetics and selectivity of a low-voltage-activated calcium current in chick and rat sensory neurones. *Journal of Physiology* **386**, 547–570.

COOMBS, J. S., ECCLES, J. C. & FATT, P. (1955). The specific ionic conductances and the ionic movements across the motoneuronal membrane that produce the inhibitory post-synaptic potential. *Journal of Physiology* **130**, 326–373.

CULL-CANDY, S. G., MILEDI, R., TRAUTMANN, A. & UCHITEL, O. D. (1980). On the release of transmitter at normal, myasthenia gravis and myasthenic syndrome affected human end-plates. *Journal of Physiology* **299**, 621–638.

CULL-CANDY, S. G. & USOWICZ, M. M. (1989). Whole-cell current noise produced by excitatory and inhibitory amino acids in large cerebellar neurones of the rat. *Journal of Physiology* **415**, 533–553.

CULLHEIM, S. & KELLERTH, J.-O. (1981). Two kinds of recurrent inhibition of cat spinal α-motoneurones as differentiated pharmacologically. *Journal of Physiology* **312**, 209–224.

CURTIS, D. R. & JOHNSTON, G. A. R. (1974). Amino acid transmitters in the central nervous system. *Ergebnisse der Physiologie* **69**, 98–188.

DEL CASTILLO, J. & KATZ, B. (1954). Quantal components of the end-plate potential. *Journal of Physiology* **124**, 560–573.

DEL CASTILLO, J. & KATZ, B. (1956). Localization of active spots within the neuromuscular junction of the frog. *Journal of Physiology* **132**, 630–649.

DODGE, F. A. JR & RAHAMIMOFF, R. (1967). Co-operative action of calcium ions in transmitter release at the neuromuscular junction. *Journal of Physiology* **193**, 419–432.

EDWARDS, F. A., KONNERTH, A. & SAKMANN, B. (1990). Quantal analysis of inhibitory synaptic transmission in the dentate gyrus of rat hippocampal slices: a patch-clamp study. *Journal of Physiology* **430**, 213–249.

EDWARDS, F. A., KONNERTH, A., SAKMANN, B. & TAKAHASHI, T. (1989). A thin slice preparation for patch clamp recordings from neurons of the mammalian central nervous system. *Pflügers Archiv* **414**, 600–612.

EDWARDS, F.R., REDMAN, S. J. & WALMSLEY, B. (1976). Statistical fluctuations in charge transfer at Ia synapses on spinal motoneurones. *Journal of Physiology* **259**, 665–688.

FATT, P. & KATZ, B. (1952). Spontaneous subthreshold activity at motor nerve endings. *Journal of Physiology* **117**, 109–128.

FINKEL, A. S. & REDMAN, S. J. (1983). The synaptic current evoked in cat spinal motoneurones by impulses in single group Ia axons. *Journal of Physiology* **342**, 615–632.

FOX, A. P., NOWYCKY, M. C. & TSIEN, R. W. (1987). Kinetic and pharmacological properties distinguishing three types of calcium currents in chick sensory neurones. *Journal of Physiology* **394**, 149–172.

GOLD, M. R. & MARTIN, A. R. (1983). Characteristics of inhibitory post-synaptic currents in brain-stem neurones of the lamprey. *Journal of Physiology* **342**, 85–98.

GOLDMAN, D. E. (1943). Potential, impedance, and rectification in membranes. *Journal of General Physiology* **27**, 37–60.

HARTZELL, H. C., KUFFLER, S. W. & YOSHIKAMI, D. (1975). Post-synaptic potentiation: interaction between quanta of acetylcholine at the skeletal neuromuscular synapse. *Journal of Physiology* **251**, 427–463.

HODGKIN, A. L. & HOROWICZ, P. (1959). The influence of potassium and chloride ions on the membrane potential of single muscle fibres. *Journal of Physiology* **148**, 127–160.

HODGKIN, A. L. & KATZ, B. (1949). The effect of sodium ions on the electrical activity of the giant axon of the squid. *Journal of Physiology* **108**, 37–77.

HUBBARD, J. I., JONES, S. F. & LANDAU, E. M. (1968). On the mechanism by which calcium and magnesium affect the spontaneous release of transmitter from mammalian motor nerve terminals. *Journal of Physiology* **194**, 355–380.

INAGAKI, C., ODA, W., KONDO, K. & KUSUMI, M. (1987). Histochemical demonstration of Cl^--ATPase in rat spinal motoneurons. *Brain Research* **419**, 375–378.

ITO, M., KOSTYUK, P. G. & OSHIMA, T. (1962). Further study on anion permeability of inhibitory post-synaptic membrane of cat motoneurones. *Journal of Physiology* **164**, 150–156.

JACK, J. J. B., REDMAN, S. J. & WONG, K. (1981). The components of synaptic potentials in cat spinal motoneurones by impulses in single group Ia afferents. *Journal of Physiology* **321**, 65–96.

KATZ, B. & MILEDI, R. (1963). A study of spontaneous miniature potentials in spinal motoneurones. *Journal of Physiology* **168**, 389–422.

KATZ, B. & MILEDI, R. (1972). The statistical nature of the acetylcholine potential and its molecular components. *Journal of Physiology* **224**, 665–699.

KOJIMA, H. & TAKAHASHI, T. (1985). Characterization of miniature inhibitory post-synaptic potentials in rat spinal motoneurones. *Journal of Physiology* **368**, 627–640.

KORN, H., BURNOD, Y. & FABER, D. S. (1987). Spontaneous quantal currents in a central neuron match predictions from binomial analysis of evoked responses. *Proceedings of the National Academy of Sciences of the USA* **84**, 5981–5985.

KUNO, M. (1964). Quantal components of excitatory synaptic potentials in spinal motoneurones. *Journal of Physiology* **175**, 81–99.

KUNO, M. (1971). Quantum aspects of central and ganglionic synaptic transmission in vertebrates. *Physiological Reviews* **51**, 647–678.

KUNO, M. & TAKAHASHI, T. (1986). Effects of calcium and magnesium on transmitter release at Ia synapses of rat spinal motoneurones *in vitro*. *Journal of Physiology* **376**, 543–553.

KUNO, M. & WEAKLY, J. N. (1972). Quantal components of the inhibitory synaptic potential in spinal motoneurones of the cat. *Journal of Physiology* **224**, 287–303.

MERCURI, N. B., CALABRESI, P. & BERNARDI, G. (1988). Potassium ions play a role in the glycine-induced inhibition of rat substantia nigra zona compacta neurones. *Brain Research* **462**, 199–203.

PUSCH, M. & NEHER, E. (1988). Rates of diffusional exchange between small cells and a measuring patch pipette. *Pflügers Archiv* **411**, 204–211.

REDMAN, S. (1990). Quantal analysis of synaptic potentials in neurons of the central nervous system. *Physiological Reviews* **70**, 165–198.

ROBINSON, R. A. & STOKES, R. H. (1959). *Electrolyte Solutions*. Butterworths, London.

ROPERT, N., MILES, R. & KORN, H. (1990). Characteristics of miniature inhibitory postsynaptic currents in CA1 pyramidal neurones of rat hippocampus. *Journal of Physiology* **428**, 707–722.

SAKMANN, B. & BRENNER, H. R. (1978). Change in synaptic channel gating during neuromuscular development. *Nature* **276**, 401–402.

SCHURR, A., WEST, C. A. & RIGOR, B. M. (1988). Lactate-supported synaptic function in the rat hippocampal slice preparation. *Science* **240**, 1326–1328.

STUART, G. J. & REDMAN, S. J. (1990). Voltage dependence of Ia reciprocal inhibitory currents in cat spinal motoneurones. *Journal of Physiology* **420**, 111–125.

TAKAHASHI, T. (1978). Intracellular recording from visually identified motoneurons in rat spinal cord slices. *Proceedings of the Royal Society* B **202**, 417–421.

TAKAHASHI, T. (1984). Inhibitory miniature synaptic potentials in rat motoneurons. *Proceedings of Royal Society* B **221**, 103–109.

TAKAHASHI, T. (1990*a*). The ionic basis of the inhibitory postsynaptic currents recorded from rat spinal motoneurons. *Japanese Journal of Physiology* **40**, suppl., 116.

TAKAHASHI, T. (1990*b*). Membrane currents in visually identified motoneurones of neonatal rat spinal cord. *Journal of Physiology* **423**, 27–46.

TAKAHASHI, T. & MOMIYAMA, A. (1991). Single-channel currents underlying glycinergic inhibitory postsynaptic responses in spinal neurons. *Neuron* **7**, 965–969.

WALMSLEY, B., EDWARDS, F. R. & TRACY, D. J. (1988). Nonuniform release probabilities underlie quantal synaptic transmission at a mammalian excitatory central synapse. *Journal of Neurophysiology* **60**, 889–908.

WALMSLEY, B. & NICOL, M. J. (1991). The effects of Ca^{2+}, Mg^{2+} and kynurenate on primary afferent synaptic potentials evoked in cat spinal cord neurones *in vivo*. *Journal of Physiology* **433**, 409–420.

WERMAN, R., DAVIDOFF, R. A. & APRISON, M. H. (1968). Inhibitory action of glycine on spinal neurons in the cat. *Journal of Neurophysiology* **31**, 81–95.

YAMAMOTO, C., HIGASHIMA, M., SAWADA, S. & KAMIYA, H. (1991). Quantal components of the synaptic potential induced in hippocampal neurons by activation of granule cells, and the effect of 2-amino-4-phosphonobutyric acid. *Hippocampus* **1**, 93–106.